## **Electrical properties and interface** abruptness of AlSiO gate dielectric grown on $(000\overline{1})$ N-polar and (0001) Ga-polar GaN

Cite as: Appl. Phys. Lett. 115, 172104 (2019); https://doi.org/10.1063/1.5125788 Submitted: 26 August 2019 . Accepted: 14 October 2019 . Published Online: 22 October 2019

Islam Sayed 🗓, Bastien Bonef 🗓, Wenjian Liu 🗓, Silvia Chan 🗓, Jana Georgieva, James S. Speck, Stacia Keller, and Umesh K. Mishra







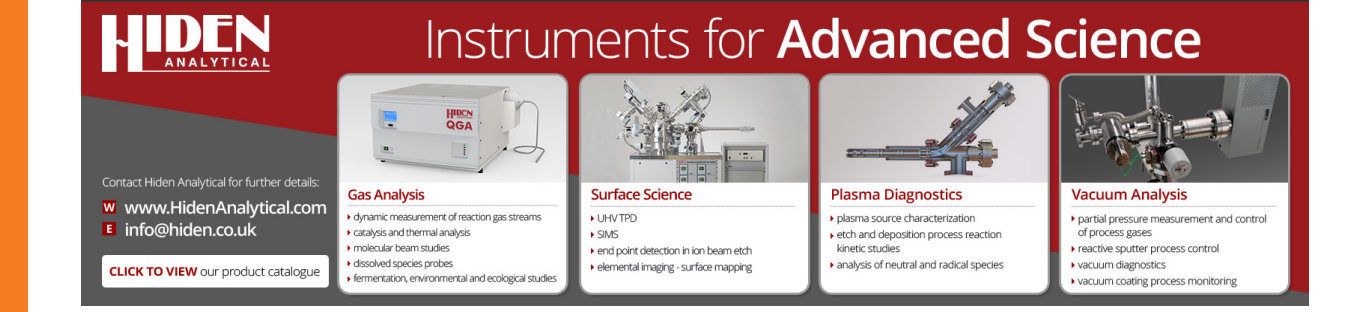
### ARTICLES YOU MAY BE INTERESTED IN

Investigation of nitrogen polar p-type doped  $GaN/Al_xGa_{(1-x)}N$  superlattices for applications in wide-bandgap p-type field effect transistors

Applied Physics Letters 115, 172105 (2019); https://doi.org/10.1063/1.5124326

Boosting the doping efficiency of Mg in p-GaN grown on the free-standing GaN substrates Applied Physics Letters 115, 172103 (2019); https://doi.org/10.1063/1.5124904

Net negative fixed interface charge for Si<sub>3</sub>N<sub>4</sub> and SiO<sub>2</sub> grown in situ on 000-1 N-polar GaN Applied Physics Letters 115, 032103 (2019); https://doi.org/10.1063/1.5111148





# Electrical properties and interface abruptness of AlSiO gate dielectric grown on $(000\overline{1})$ N-polar and (0001) Ga-polar GaN

Cite as: Appl. Phys. Lett. **115**, 172104 (2019); doi: 10.1063/1.5125788 Submitted: 26 August 2019 · Accepted: 14 October 2019 · Published Online: 22 October 2019







Islam Sayed,<sup>1,a)</sup> D Bastien Bonef,<sup>2</sup> Wenjian Liu,<sup>1</sup> D Silvia Chan,<sup>2</sup> D Jana Georgieva,<sup>1</sup> James S. Speck,<sup>2</sup> Stacia Keller,<sup>1</sup> and Umesh K. Mishra<sup>1</sup>

#### **AFFILIATIONS**

Department of Electrical and Computer Engineering, University of California, Santa Barbara, California 93106, USA

#### **ABSTRACT**

The electrical properties and the interface abruptness of aluminum silicon oxide (AlSiO) dielectric grown in situ on  $(000\overline{1})$  N-polar and (0001) Ga-polar GaN by metal organic chemical vapor deposition were studied by means of capacitance-voltage (CV) and atom probe tomography (APT) measurements. The growth of AlSiO on N-polar GaN resulted in a positive flatband voltage shift of 2.27 V with respect to that on Ga-polar GaN, which exemplifies the influence of the GaN surface polarization charge on the electrical properties of GaN-based metal oxide semiconductor (MOS) devices. The AlSiO/GaN(N-polar) interface was sharp, which resulted in nondispersive CV characteristics and a relatively low density of interface states ( $D_{it}$ ) of  $1.48 \times 10^{12}$  cm<sup>-2</sup>. An intermixed layer of AlGaSiO was present at the interface between AlSiO and Ga-polar GaN, which contributed to the measured dispersive CV characteristics and resulted in an  $\sim 2\times$  higher  $D_{it}$  than that on N-polar GaN. The superior properties of the N-polar AlSiO MOS devices are promising for further advancement of N-polar GaN-based high electron mobility transistors for high-frequency and power electronics applications.

Published under license by AIP Publishing. https://doi.org/10.1063/1.5125788

Aluminum silicon oxide (AlSiO) has been proposed recently as a promising high-quality insulator that can improve the gate robustness of GaN-based metal oxide semiconductor (MOS) devices. 1,2 Studies have shown that alloying of Al<sub>2</sub>O<sub>3</sub> with Si led to high amorphous stability and improved bulk and interfacial properties compared to Al<sub>2</sub>O<sub>3</sub>.<sup>3,4</sup> In addition, recent findings showed that the high bulk/ interface quality of AlSiO resulted in a predicted lifetime of 20 years for electric fields higher than 3 MV/cm and a low interface state density ( $D_{it}$ ) of  $\sim 10^{12}$  cm $^{-2.5}$  Compared to  $Al_2O_3$ , AlSiO has a higher conduction band offset to GaN, which resulted in lower leakage current.<sup>2</sup> All previous research studies on AlSiO focused primarily on evaluating its electrical and structural properties on Ga-polar GaN. 1,2,4 Recently, GaN-based high electron mobility transistors (HEMTs) based on the N-polar technology have demonstrated high-performance millimeter-wave amplifiers and power devices. 6.7 The advancements of the N-polar technology over the Ga-polar technology motivated evaluating the electrical and structural properties of AlSiO on N-polar GaN and studying the impact of GaN polarity to further improve the gate-robustness of N-polar HEMTs.

In this paper, the electrical properties and interface abruptness of AlSiO grown on N-polar and Ga-polar GaN are compared by means of capacitance-voltage (CV) and atom probe tomography (APT) measurements. We demonstrate that the growth of AlSiO on N-polar GaN resulted in a positive flatband voltage shift of 2.27 V with respect to that on Ga-polar GaN, which exemplifies the impact of GaN surface polarization charge on the properties of GaN-based MOS devices. The interface between the AlSiO layer and the N-polar GaN layer was sharp, which contributed to the measured nondispersive CV characteristics and a relatively low  $D_{it}$  of  $1.48 \times 10^{12} \, \mathrm{cm}^{-2}$ . On the other hand, high intermixing between oxygen, gallium, and aluminum occurred at the interface between the AlSiO layer and the Ga-polar GaN layer, which contributed to the measured dispersive CV characteristics and relatively high  $D_{it}$  of  $3.1 \times 10^{12} \, \mathrm{cm}^{-2}$ .

The insulator-semiconductor structures were grown in a closed coupled showerhead metal organic chemical vapor deposition (MOCVD) reactor. The N-polar epitaxial structure was grown on a c-plane sapphire substrate misoriented by  $4^{\circ}$  toward the a-plane, and the structure consisted of, from bottom to top,  $0.5~\mu m$  unintentionally

<sup>&</sup>lt;sup>2</sup>Materials Department, University of California, Santa Barbara, California 93106, USA

<sup>&</sup>lt;sup>a)</sup>islam\_sayed@ucsb.edu

doped GaN ( $9 \times 10^{17}~{\rm cm}^{-3}$ ), 0.8  $\mu m$  n+ GaN ( $2.5 \times 10^{18}~{\rm cm}^{-3}$ ), and 0.6  $\mu m$  n-GaN ( $2.5 \times 10^{17}~{\rm cm}^{-3}$ ). The Ga-polar epitaxial structure was grown on on-axis c-plane sapphire substrates and consisted of, from bottom to top, 1  $\mu m$  semi-insulating GaN, 0.6  $\mu m$  unintentionally doped GaN ( $\sim 6 \times 10^{15}~{\rm cm}^{-3}$ ), 0.8  $\mu m$  n+GaN ( $2.5 \times 10^{18}~{\rm cm}^{-3}$ ), and 0.6  $\mu m$  n-GaN ( $2.5 \times 10^{17}~{\rm cm}^{-3}$ ). The N-polar and Ga-polar GaN epitaxial structures were capped *in situ* by AlSiO with a thickness of  $\sim 23$  nm grown by MOCVD at 700 °C. Metal-oxide-semiconductor capacitors (MOSCAPs) were processed as mesa structures using plasma reactive ion etching, and Ti/Au metal stack was deposited as both the Ohmic contact on the n+ GaN and the gate contact on the dielectric.

APT was used to evaluate the alloy distribution in the AlSiO layers and to study the impact of GaN polarity on the interface abruptness between AlSiO and GaN. 8,9 For APT evaluation, a 160 nm GaN cap layer was grown at 630 °C on top of the AlSiO, which aided the APT tip fabrication and produced more reliable APT data. 10 The APT tips were prepared using an FEI Helios 600 dual-beam focused ion beam (FIB) instrument following the standard procedure. 11 The APT measurements were performed using a Cameca 3000X HR Local Electrode Atom Probe (LEAP) operating in laser-pulse mode (13 ps pulse, 532 nm green laser, 10  $\mu$ m laser spot size). The same evaporation parameters were applied to study both samples. A base temperature of 60 K and a laser pulse intensity of 1 nJ were used. A detection rate of 0.005 atoms/pulse was set during the measurements. APT 3D reconstructions were carried out using commercial software  $\mbox{IVAS}^{\mbox{\scriptsize TM}}$ following a geometrical based algorithm. 12 Reconstruction parameters were iteratively optimized based on the AlSiO layer thicknesses measured by X-ray reflectivity measurements.

The 1D concentration profiles of Al, O, and Ga along the growth direction for the N-polar sample and the Ga-polar sample are shown in Figs. 1(a) and 1(b), respectively. The profiles were measured in  $20 \times 20 \times 30 \, \mathrm{nm^3}$  sampling volumes extracted in the center of the 3D APT reconstructions. Because of the mass overlap of Si and N based ions in the APT mass spectrum, these two elements were not considered in the regions far away from the AlSiO/GaN interface. Consequently, it is expected to measure a 100% Ga concentration in the bottom and top GaN layers. Composition measurements for both layers are marked by the gray areas shown in Figs. 1(a) and 1(b). These volumes were chosen because no concentration gradients in the growth direction were observed in this region. The obtained concentrations for the N-polar sample were 7% of Si, 55% of O, 36% of Al,

and 2% of C. For the Ga-polar sample, 4% of Si, 54% of O, 40% of Al, and 2% of C were measured.

The alloy distributions in the AlSiO layers for both samples were investigated from the APT sampling volumes shown in the gray areas in Figs. 1(a) and 1(b). Radial distribution analysis (RDA) was used to detect the presence of phase separation. 13,14 The ratio of the composition found in spherical shells around each atom to the overall sample composition is plotted vs the shell radius in Figs. 1(c) and 1(d). The self-correlation technique is based on measuring the compositions of atoms of chemical nature A with respect to a chemically identical A atom being in the center of the shell. In the cross correlation technique, the compositions of atoms of chemical nature B with respect to a chemically different A atom being in the center of the shell are measured. Ratios above 1 in these curves at short distances would indicate phase separation. Here, all possible combinations of atoms relative to Al, O, and Si atoms are plotted in Fig. 1(c) for the N polar sample and Fig. 1(d) for the Ga polar sample. For both samples, all curves remain close to a value of 1, indicating the absence of phase separation in the AlSiO layers.

The bottom interfaces between the AlSiO and the GaN layers were evaluated and compared between the two samples using the 1D concentration profile in Figs. 1(a) and 1(b). In Fig. 1(a), for the N-polar sample, the AlSiO/GaN interface is sharp. A thickness transition of only 1.8 nm from a Ga percentage of 90 to 10 was measured in the growth direction. On the other hand, this transition takes 4.8 nm for the Ga-polar sample in Fig. 1(b). The interface region between the Ga-polar GaN layer and the AlSiO layer can be considered as a separate intermixed layer of AlGaSiO. To confirm the presence of Ga in this specific region of the Ga-polar sample, a sampling volume corresponding to the orange area in Fig. 1(b) was chosen for 3D APT reconstruction. This mass spectrum is shown in Fig. 2. Ions corresponding to the expected evaporations of Al, Si, and O can be clearly identified. It is also clear from the mass spectrum that  $Ga_{69}^{++}$  (mass/q equal to 34.5),  $\operatorname{Ga}_{71}^{++}$  (mass/q equal to 35.5),  $\operatorname{Ga}_{69}^{+}$  (mass/q equal to 69), and  $Ga_{71}^+$  (mass/q equal to 71) ions are also detected confirming the presence of Ga in the interlayer.

The electrical properties of the N-polar and Ga-polar AlSiO MOSCAP devices were investigated using CV measurements. The CV data of N-polar and Ga-polar GaN devices, measured at 100 kHz, are depicted in Fig. 3. The accumulation capacitance in both AlSiO samples was  $\sim\!0.26~\mu\text{F/cm}^2$ , and the extracted dielectric constant of AlSiO was  $\sim\!6.7$ . The flatband voltages were extracted from the CV curves at

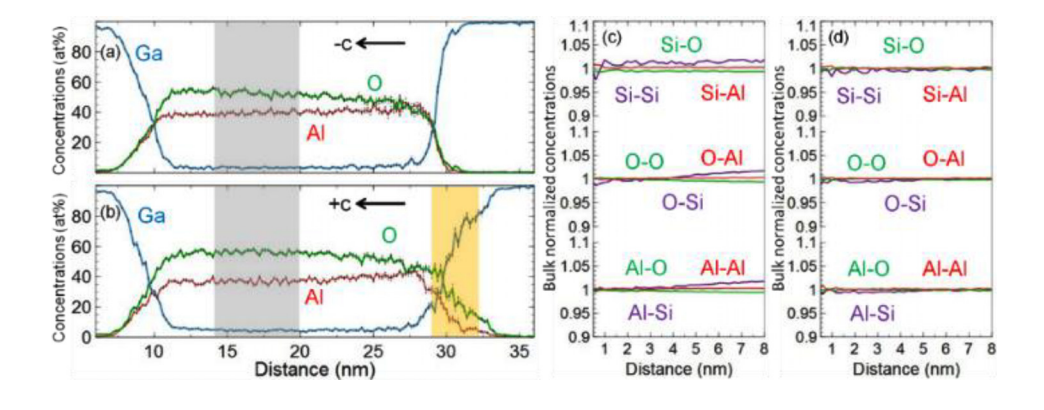


FIG. 1. 1D concentration profiles of AI, O, and Ga along the growth direction and taken from the APT 3D reconstruction of (a) the N-polar sample and (b) the Ga-polar sample. Respective radial distribution analyses showing cross correlation and self-correlation values for AI, O, and Si atoms for (c) the N-polar sample and (d) the Ga-polar sample in sampling volumes extracted from the gray regions in (a) and (b).

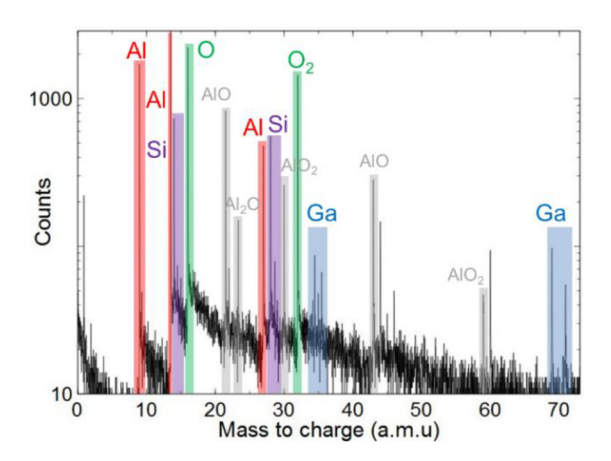


FIG. 2. APT mass spectrum measured from 0 to 73 atomic mass units and in the sampling volume defined as the orange region in Fig. 1(b).

the flatband capacitance using the methodology described in Ref. 15. The flatband voltages of AlSiO on N-polar and Ga-polar GaN were -1.61 V and -3.88 V, respectively. The presence of a positive flatband voltage shift of 2.27 V for the N-polar device with respect to the Gapolar device indicated that the net fixed charges located at the AlSiO/ GaN interface for the two samples were significantly different. Due to the absence of inversion symmetry in the GaN crystals, positive and negative polarization charges exist on the surface of N-polar and Gapolar GaN, respectively. 16 Studies on MOCVD-grown Al<sub>2</sub>O<sub>3</sub>, Si<sub>3</sub>N<sub>4</sub>, and SiO<sub>2</sub> showed that compensating negative and positive charges are present at the dielectric/GaN(N-polar) and dielectric/GaN(Ga-polar) interfaces, respectively. 17-19 This polarity-dependent interface charge can affect the sign and the magnitude of the flatband voltage. The accurate measurement of the net interface charge for the AlSiO samples presented here requires analyzing devices with various thicknesses to eliminate the effects from the trapped charges,<sup>20</sup> which was not the focus of this study and will be pursued in the future.

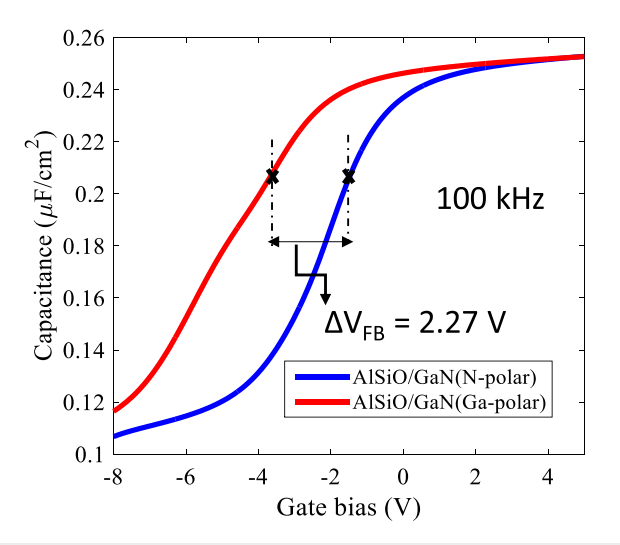
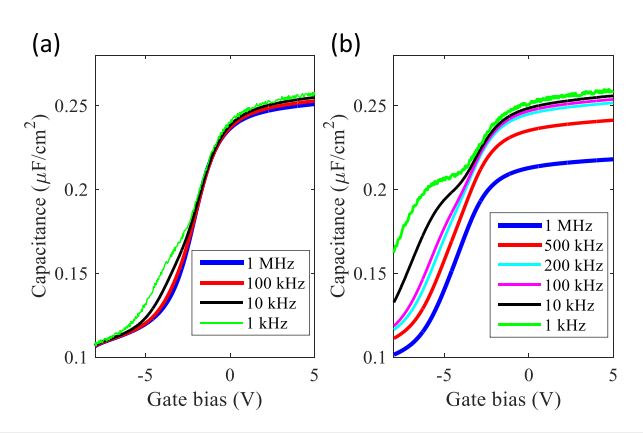


FIG. 3. Capacitance-voltage characteristics of AlSiO on N-polar GaN and AlSiO on Ga-polar GaN MOSCAP devices, measured at 100 kHz.



**FIG. 4.** Frequency-dependent CV characteristics of (a) AlSiO on the N-polar GaN MOSCAP device and (b) AlSiO on the Ga-polar GaN MOSCAP device.

The frequency-dependent CV characteristics of AlSiO on N- and Ga-polar GaN MOSCAPs are shown in Figs. 4(a) and 4(b), respectively. At a given frequency, traps with an energy level close to the Fermi level and with emission times shorter than the inverse of the operating frequency are expected to respond to the applied ac signal and contribute to additional capacitance. The CV behavior in Fig. 4 clearly shows two distinguishable regions for each device. The first region is where border traps can contribute to additional capacitance for an applied voltage bias beyond accumulation. 21,22 The second region is where interface states are mostly stimulated for an applied voltage bias between weak depletion and the onset of accumulation.<sup>21</sup> CV frequency dispersion was clearly observed for the Ga-polar sample, which indicated that there was a higher density of border traps and interface trap states probably due to the presence of large Al-Ga-O intermixing as shown in the APT results of Figs. 1(b) and 2. In contrast, the frequency dispersion of the N-polar MOSCAP was significantly less, thus suggesting improved interface quality with lower interface

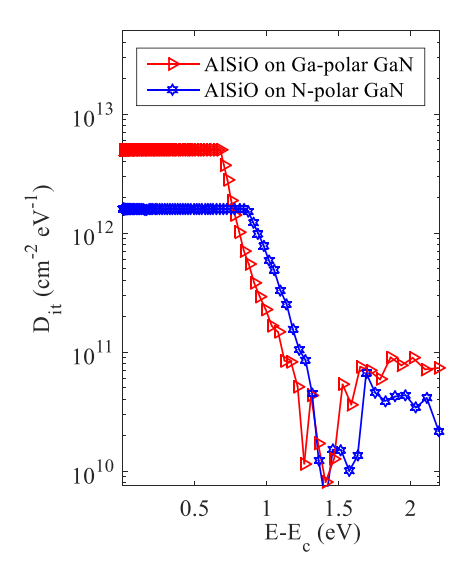


FIG. 5. Interface state distribution of AlSiO on N-polar GaN and AlSiO on Ga-polar GaN MOSCAP devices.

states probably due to the presence of a sharp interface between AlSiO and N-polar GaN as shown in Fig. 1(a).

For a more quantitative analysis on the interface trap distribution, the photoassisted CV method was used, which employs ultraviolet (UV) illumination to generate electron-hole pairs that can recombine via interface state mediated hole capture. <sup>23</sup>  $D_{ib}$  shown in Fig. 5, was extracted through analyzing the CV curves measured in the dark before and after the UV exposure. <sup>23</sup> Due to the presence of a positive valence band barrier, the holes present at the interface between GaN and AlSiO can affect the UV-assisted CV measurement, and the analysis described in Ref. 24 was followed in order to extract the  $D_{it}$  accurately. The integrated  $D_{it}$  values for the Ga-polar and N-polar MOSCAPs were  $3.1 \times 10^{12}$  cm<sup>-2</sup> and  $1.48 \times 10^{12}$  cm<sup>-2</sup>, respectively. The  $D_{it}$  value of the Ga-polar MOSCAP was about double that of the N-polar MOSCAP, probably related to the high Al-O-Ga intermixing that was observed for the Ga-polar sample. The superior electrical properties of the N-polar AlSiO MOSCAPs presented in this article are promising for further enhancement of the gate robustness of N-polar GaN-based HEMTs.

To conclude, by means of atom probe tomography and capacitance-voltage measurements, the interface abruptness and the electrical properties of AlSiO grown *in situ* on N-polar and Ga-polar GaN were investigated. The properties of the Ga- and N-polar MOSCAPs exhibited distinct differences, with  $D_{it}$  at the interface between AlSiO and Ga-polar GaN being about double compared to that between AlSiO and N-polar GaN. In addition, the dispersion in the CV characteristics was more significant for the AlSiO Ga-polar MOSCAPs than the AlSiO N-polar MOSCAPs. The superior properties of the N-polar AlSiO MOSCAPs are promising for further advancement of N-polar GaN-based HEMTs.

The authors acknowledge the financial support of the Office of Naval Research (monitored by Dr. Paul Maki), the Simons Foundation (No. 601952, JS), and the NSF RAISE-TAQS Program No. 1839077 through a subcontract from the University of Minnesota.

#### **REFERENCES**

- <sup>1</sup>S. H. Chan, M. Tahhan, X. Liu, D. Bisi, C. Gupta, O. Koksaldi, H. Li, T. Mates, S. P. DenBaars, and S. Keller, "Metalorganic chemical vapor deposition and characterization of (Al, Si) O dielectrics for GaN-based devices," Jpn. J. Appl. Phys., Part 1 55, 021501 (2016).
- <sup>2</sup>D. Kikuta, K. Itoh, T. Narita, and T. Mori, "Al<sub>2</sub>O<sub>3</sub>/SiO<sub>2</sub> nanolaminate for a gate oxide in a GaN-based MOS device," J. Vac. Sci. Technol., A **35**, 01B122 (2017).
- <sup>3</sup>N. Komatsu, K. Masumoto, H. Aoki, C. Kimura, and T. Sugino, "Characterization of Si-added aluminum oxide (AlSiO) films for power devices," Appl. Surf. Sci. 256, 1803–1806 (2010).
- <sup>4</sup>S. H. Chan, S. Keller, O. S. Koksaldi, C. Gupta, S. P. DenBaars, and U. K. Mishra, "Exploring metalorganic chemical vapor deposition of Si-alloyed Al<sub>2</sub>O<sub>3</sub> dielectrics using disilane," J. Cryst. Growth 464, 54–58 (2017).
- <sup>5</sup>S. Chan, "First developments of AlSiO gate dielectrics by MOCVD: A pathway to efficient GaN electronics," Ph.D. dissertation (UC Santa Barbara, 2018).

- <sup>6</sup>O. S. Koksaldi, J. Haller, H. Li, B. Romanczyk, M. Guidry, S. Wienecke, S. Keller, and U. K. Mishra, "N-Polar GaN HEMTs Exhibiting Record Breakdown Voltage Over 2000 V and Low Dynamic On-Resistance," IEEE Electron Device Lett. **39**(7), 1014–1017 (2018).
- <sup>7</sup>B. Romanczyk, S. Wienecke, M. Guidry, H. Li, E. Ahmadi, X. Zheng, S. Keller, and U. K. Mishra, "Demonstration of constant 8 W/mm power density at 10, 30, and 94 GHz in state-of-the-art millimeter-wave N-polar GaN MISHEMTS," IEEE Trans. Electron Devices 65, 45–50 (2018).
- <sup>8</sup>H. Li, B. Mazumder, B. Bonef, S. Keller, S. Wienecke, J. S. Speck, S. P. Denbaars, and U. K. Mishra, "Characterization of N-polar AlN in GaN/AlN/ (Al, Ga) N heterostructures grown by metal-organic chemical vapor deposition," Semicond. Sci. Technol. 32, 115004 (2017).
- <sup>9</sup>B. Mazumder, M. Wong, C. Hurni, J. Zhang, U. Mishra, and J. Speck, "Asymmetric interfacial abruptness in N-polar and Ga-polar GaN/AlN/GaN heterostructures," Appl. Phys. Lett. **101**, 091601 (2012).
- <sup>10</sup>B. Mazumder, X. Liu, R. Yeluri, F. Wu, U. K. Mishra, and J. S. Speck, "Atom probe tomography studies of Al<sub>2</sub>O<sub>3</sub> gate dielectrics on GaN," J. Appl. Phys. 116, 134101 (2014).
- <sup>11</sup>K. Thompson, D. Lawrence, D. Larson, J. Olson, T. Kelly, and B. Gorman, "In situ site-specific specimen preparation for atom probe tomography," Ultramicroscopy 107, 131–139 (2007).
- <sup>12</sup>F. Vurpillot, B. Gault, B. P. Geiser, and D. Larson, "Reconstructing atom probe data: A review," Ultramicroscopy 132, 19–30 (2013).
- <sup>13</sup>B. Bonef, S. D. Harrington, D. J. Pennachio, J. S. Speck, and C. J. Palmstrøm, "Nanometer scale structural and compositional inhomogeneities of half-Heusler CoTi1-xFexSb thin films," J. Appl. Phys. 125, 205301 (2019).
- <sup>14</sup>J. Zhou, J. Odqvist, M. Thuvander, and P. Hedström, "Quantitative evaluation of spinodal decomposition in Fe-Cr by atom probe tomography and radial distribution function analysis," Microsc. Microanal. 19, 665–675 (2013).
- 15 U. Mishra and J. Singh, Semiconductor Device Physics and Design (Springer Science & Business Media, 2007).
- <sup>16</sup>B. S. Eller, J. Yang, and R. J. Nemanich, "Polarization effects of GaN and AlGaN: Polarization bound charge, band bending, and electronic surface states," J. Electron. Mater. 43, 4560–4568 (2014).
- <sup>17</sup>I. Sayed, W. Liu, S. Chan, C. Gupta, M. Guidry, H. Li, S. Keller, and U. Mishra, "Net negative fixed interface charge for Si<sub>3</sub>N<sub>4</sub> and SiO<sub>2</sub> grown in situ on 000–1 N-polar GaN," Appl. Phys. Lett. 115, 032103 (2019).
- <sup>18</sup>X. Liu, J. Kim, D. Suntrup, S. Wienecke, M. Tahhan, R. Yeluri, S. Chan, J. Lu, H. Li, and S. Keller, "In situ metalorganic chemical vapor deposition of Al<sub>2</sub>O<sub>3</sub> on N-face GaN and evidence of polarity induced fixed charge," Appl. Phys. Lett. 104, 263511 (2014).
- <sup>19</sup>X. Liu, C. Jackson, F. Wu, B. Mazumder, R. Yeluri, J. Kim, S. Keller, A. Arehart, S. Ringel, and J. Speck, "Electrical and structural characterizations of crystal-lized Al<sub>2</sub>O<sub>3</sub>/GaN interfaces formed by in situ metalorganic chemical vapor deposition," J. Appl. Phys. 119, 015303 (2016).
- <sup>20</sup>D. K. Schroder, Semiconductor Material and Device Characterization (John Wiley & Sons, 2006).
- <sup>21</sup>Y. Yuan, B. Yu, J. Ahn, P. C. McIntyre, P. M. Asbeck, M. J. Rodwell, and Y. Taur, "A Distributed Bulk-Oxide Trap Model for Al<sub>2</sub>O<sub>3</sub> InGaAs MOS Devices," IEEE Trans. Electron Devices 59, 2100–2106 (2012).
- <sup>22</sup>H.-P. Chen, J. Ahn, P. C. McIntyre, and Y. Taur, "Effects of oxide thickness and temperature on dispersions in InGaAs MOS CV characteristics," J. Vac. Sci. Technol., B 32, 03D111 (2014).
- 23B. Swenson and U. Mishra, "Photoassisted high-frequency capacitance-voltage characterization of the Si<sub>3</sub>N<sub>4</sub>/GaN interface," J. Appl. Phys. 106, 064902 (2009).
- <sup>24</sup>R. Yeluri, X. Liu, B. L. Swenson, J. Lu, S. Keller, and U. K. Mishra, "Capacitance-voltage characterization of interfaces between positive valence band offset dielectrics and wide bandgap semiconductors," J. Appl. Phys. 114, 083718 (2013).